HHS Public Access

Author manuscript

FEBS Lett. Author manuscript; available in PMC 2016 April 02.

Published in final edited form as:

FEBS Lett. 2015 April 2; 589(8): 885–889. doi:10.1016/j.febslet.2015.02.030.

Acquiring Snapshots of the Orientation of Trans-membrane Protein Domains Using a Hybrid FRET Pair

Robert F. Gahl[1], **Ephrem Tekle**[1], **Gefei Alex Zhu**, **Justin W. Taraska**, and **Nico Tjandra**[*]

Biochemistry and Biophysics Center, Laboratory of Molecular Biophysics; National Heart, Lung and Blood Institute, National Institutes of Health, 50 South Drive, Bethesda, Maryland 20892, United States of America

Abstract

One challenge in studying the function of membrane-embedded proteins is determining the orientation of key domains in the context of the changing and dynamic membrane environment. We describe a confocal microscopy setup that utilizes external electric field pulses to direct dipicrylamine (DPA) to a membrane leaflet. The detection of FRET between DPA and a fluorescent probe attributes it to the inner or outer leaflet of a membrane. By utilizing short acquisition times and confocal imaging, this attribution could be made even in changing membrane environments. Our setup adds versatility to the study of the biological activity of membrane-embedded proteins.

Keywords

Fluorescence; Förster Resonance Energy Transfer (FRET); Confocal Microscopy; Membrane Proteins; Live Cells; Giant Unilamellar Vesicles (GUV)

INTRODUCTION

Membrane-inserted proteins are key components in various cellular processes including signal transduction, cell-cell adhesion, and the import and export of cellular components. Determining the orientation of transmembrane domains of these proteins is critical to the understanding of their function[1,2]. The preparation of membranes selectively enriched with small molecule reporters on either the inner or outer leaflet has been utilized to identify which portion of the protein is in the intra- or extracellular side[3-5]. Recently, Dipicrylamine (DPA), a non-fluorescent lipophilic anion, has been used to preferentially occupy either leaflet[6,7]. DPA can act as a FRET acceptor through dipolar interactions with fluorescent dyes conjugated to specific locations in an embedded protein. It can be targeted to the inner

Corresponding Author USA Phone: (301) 402-3029, Fax: (301) 402-3405, tjandran@nhlbi.nih.gov.

[1]These authors contributed equally to this work.

or outer leaflet of a membrane by applying an electric field[8,9]. Therefore, a loss of fluorescent signal associated with a certain polarity of the electric field can indicate the leaflet where this specific site on a protein resides. This control over the differentiation of the inner and outer leaflets of these membranes has been applied to determining the orientation of transmembrane domains in pore-forming proteins embedded in lipid bilayer systems[9,10]. Biological membranes, however can undergo dramatic changes that can induce the formation of microdomains in response to stimuli, which can act as a scaffold to form protein complexes[11]. A bulk or average measurement of the conformation of proteins over large areas of the membrane may not be sufficient to characterize their biological activity. Therefore, we demonstrate a method that utilizes DPA with added versatility to extract details about the orientation of transmembrane domains from small regions of interest that can be associated with different morphological features on synthetic or biological membranes in a matter of seconds.

Figure 1 illustrates how changes in the signal from a fluorophore due to FRET with DPA can be used to identify which leaflet it occupies. DPA can diffuse freely in the core of the membrane environment where a fluorophore is embedded in a particular leaflet, Figure 1A. The application of a pulsed electric field causes DPA to migrate parallel with the direction of the field. Depending on the orientation of the membrane with the electric field, Figure 1B, the intensity of the fluorophore can change differently, Figure 1C. The location of DPA does not change in regions perpendicular to the electric field, therefore the intensity of the fluorophore will not be affected. The geometric orientation of the membrane environment is determined from confocal images to correctly interpret changes in intensity as a function of the applied electric field.

With an appropriate electrodes setup we established a geometric dependence of the electric field relative to a membrane environment. This was confirmed using Di-8-ANEPPS, a fast responding electrochromic dye, as a reporter of membrane potential. This electric field correctly manipulated DPA in live cells to identify fluorophores preferentially populated in the inner and outer leaflet of the plasma membrane. Finally, the orientation of a transmembrane domain of the pore-forming protein, Bax, was determined in giant unilamellar vesicles (GUV). Bax is a pro-apoptotic member of the Bcl-2 family of proteins that creates pores in the outer-mitochondrial membrane (OMM) at the onset of apoptosis[12]. While there have been studies that have extracted structural information about membrane-embedded Bax[12-15], the orientation of certain helices within a membrane environment have been difficult to determine without imposing some assumptions. Our setup is able to rapidly assign an orientation of a transmembrane helix within small regions of interest on the vesicle free of assumptions with a minimal number of experiments. These results illustrated the added versatility and clarity in studying membrane-embedded proteins using this approach.

MATERIALS AND METHODS

A detailed description of the materials and methods can be found in the “Supplementary Information”.

RESULTS AND DISCUSSION

It is important to first establish that we could generate an electric potential that varies as a function of location on the membrane. The Di-8-ANEPPS, a fast responding electrochromic dye, is a good reporter for membrane potential[16] and is ideal for this application. Figure 2 demonstrates the dependence of a Di-8-ANEPPS fluorescence on our applied electric field detected by confocal microscopy. The magnitude and the spatial distribution of field induced transmembrane potential ($\Delta\phi_i$) can be measured using Di-8-ANEPPS embedded in the outer-membrane of PC12 cells. Electric field effects on the fluorescence intensity are represented as a fractional fluorescence change, $\Delta F/F$. ΔF is defined as (F_S-F), where F_S is the mean fluorescence in the presence of the electric field and F is the mean fluorescence before the application of the field.

The dye exhibits an increase or decrease in fluorescence intensity following hyperpolarizing and depolarizing pulses, respectively. Figure 2A shows a fluorescence image of a PC12 cell stained with Di-8-ANEPPS. The relative positions of the electrodes, (+), and (-) are as shown on the top of the image panel, along with the direction of the electric field, $\boldsymbol{E}$. The position marked X on the cell membrane indicates the approximate location of a spot image scan, and serves as a reference for angular measurements. The angle θ at position X is set to 0, and other locations on the membrane are referenced going in a clockwise direction from 0° to 360°. Figure 2B shows single trace optical responses to an applied field of 166 V/cm, and a pulse-width of 20 ms for select locations on the membrane. The locations of the image scans are indicated with θ values. At θ = 0° and 180° the fractional fluorescence changes, $\Delta F/F$, were the highest at 0.345 and − 0.222, respectively. At positions perpendicular to the field (θ=90°, 270°), where the induced membrane potential $\Delta\phi_i$ =0, almost no responses were observed, as expected. Figure 2C shows the timing diagram for the experiment. When image acquisition is initiated, an external circuit creates a delay that can be varied between 50-100 ms prior to creating a trigger pulse that will be used to initiate an electric discharge with a duration of 20 ms across the cell. This way, spot-acquired images can be synchronized with pulsed electric fields.

The fractional changes in fluorescence around the cell surface under a constant applied field are plotted in Figure 2D left panel. Angular dependence of the magnitude of the field-induced membrane potential can be computed from the function[17-19], $\Delta\phi(\theta)=3/2 \bullet a \bullet E \bullet \cos(\theta)$, where a, E, and θ, are the cell radius, applied field, and solid angle between field direction and membrane surface, respectively. In Figure 2D right panel we have plotted the fractional fluorescence change against the computed induced potential at various positions on the cell surface. Error bars represent standard errors, n=3. A least-squares fit of the data shows a percentage change in fluorescence per 100 mV of induced potential of 16.9% - a value significantly better than previous reports of ~13% per 100 mV[16] and attests to the sensitivity of the optical response achieved with our current system.

To test whether our setup can determine a donor fluorophore's location at the *inner-membrane* leaflet, we used PC12 cells transfected with a plasmid encoding for farnesylated monomeric enhanced GFP (mEGFP-F) as a model system, where the farnesyl moiety targets

the fluorophore to the inner leaflet of the cell membrane. Figure 3A is the fluorescence image of mEGFP-F expressing cell.

The electrode locations are shown on the top corners of image panel and data were collected at the approximate positions marked (+) and (x) on the cell membrane corresponding to locations of maximum potential drop. Figure 3B is a bright field image of the same field of view as in Figure 3A and Figure 3C shows the structure of mEGFP-F (not in scale). In the absence of DPA, no change in fluorescence was observed after applying a 20 ms pulse of 166 V/cm electric field (Figure 3D). This response confirms that the donor fluorophore has no intrinsic sensitivity to the induced membrane potential. In Figure 3E, the cell was incubated with 10 μM DPA for ~ 5 minutes and exposed to the same field conditions. The optical signals observed are consistent with a field-dependent translocation of DPA away from the donor at the positive electrode-facing hemisphere, and towards the donor at the negative electrode-facing hemisphere, thereby accurately identifying the membrane leaflet to which the donor fluorophore is associated. Figure 3F shows averages of three single trace recordings under the same conditions as in Figure 3E. The fractional fluorescence changes, $\Delta F/F = 0.073 \pm 0.008$ at position (+) (S/N = 2.13) and $\Delta F/F = -0.117 \pm 0.009$ at position (x) (S/N=3.5). Figure 3G shows absence of FRET signals at membrane locations perpendicular to the applied field, ($\Delta\phi_i = 0$) and thus supports that the data shown in Figures 3E-F is due to field dependent DPA mobility. Loss of FRET also resulted at positions marked (×) and (+) in Figure 3A by permeabilizing the cell membrane in 0.05% Triton X-100 solution to prevent the buildup of induced membrane potential (data not shown).

Following a similar procedure discussed above, the location of a donor fluorophore on the *outer-membrane* leaflet was probed using the lipophilic membrane stain FM1-43. FM1-43 has been shown to not cross the membranes and thus labels only the outer membrane leaflet[20,21]. Figure 4A shows the fluorescence image of a PC12 cell labeled with 1 μM of FM1-43 (structure shown in Figure 4B).

As expected, no optical signal is observed in the absence of DPA (Figure 4C). The single trace FRET response in the presence of DPA is shown in Figure 4D; the signals acquired were opposite of those shown in Figure 4E, thus localizing the donor fluorophore on the outer membrane leaflet. Average of single traces (n=3) is shown in Figure 4E, with $\Delta F/F = -0.166 \pm 0.016$ (S/N = 4.7) at position (+) and $\Delta F/F = 0.165 \pm 0.0143$ (S/N = 4.8) at position (x). The fractional fluorescence change was more robust in this case, than for the mEGFP-F labeled cells, probably due to the closer location of FM1-43 to the membrane interface than would be expected for the farnesylated mEGFP construct.

After verifying that this confocal setup can correctly identify fluorescent probes that preferentially occupy inner-and outer-leaflets in membranes, this setup was also used to determine the orientation of helix six in membrane embedded protein Bax in GUVs. Single cysteine variants of Bax were conjugated to the FRET donor, AlexaFluor546, on the N- and C-terminal ends of helix six, Cys126 and Arg145Cys, respectively, using previously described methods[22]. These variants rapidly inserted to the GUVs when tBid was present. The truncated version of the protein Bid (tBid) by caspase-8 was shown to be necessary to

activate Bax for incorporation into artificial membranes[23]. Figure 5 shows the vesicles being held stationary by the Micropipette Cell Holder.

To determine which leaflet Cys126 and Arg145Cys occupies, two 20 ms pulses of opposite polarity were applied in succession. In Figure 5C, two signals are observed resulting from these two pulses. However, the sign of these two signals are different for these two mutants. Cys126 can be identified as occupying the inner-leaflet because of the positive then negative signal, while Arg145Cys occupies the outer-leaflet because of the reverse sign of the signal at the same polarity of the electric field. The lower intensity of the signal from the second pulse can be attributed to the re-equilibration of DPA when the polarity of the pulse inverts. This orientation is consistent with a previously proposed model[24] that used a cysteine-scanning method. Interestingly, another study has proposed a different orientation of this helix also using a cysteine-scanning method[13]. Using this setup, our work unambiguously assigns the orientation of helix six in a rapid measurement using only two samples. In addition, since Bax has been shown to fragment the OMM[12] and these measurements were taken rapidly before such pores were formed, we were also able to capture early membrane insertion events of Bax. It is possible that different mitochondrial environments were analyzed, which could explain the discrepancy in the two previously published studies. In our approach, if membrane topology were to undergo changes, the relative orientation of the electric field can be adjusted. As a result, a re-orientation of transmembrane domains could be detected. The short acquisition time and the ability to measure at a specific location on the membrane that are implemented in our method can provide flexibility in studying morphological changes in a membrane environment. Such data can complement additional structural information to give a more complete picture of the biological activity of membrane-embedded proteins.

CONCLUSIONS

We have described a fast and accurate optical identification of fluorophores located on the cis and trans-facing membrane leaflets using DPA as a FRET acceptor. Modulation of the membrane potential, that directs the DPA to a specific membrane leaflet, can be attained by application of an external electric field that is easily synchronized with an imaging system. Our method could be used to probe the topologies of fluorophore-labeled plasma membrane proteins and peptides in live cells and synthetic membrane systems. While there are challenges in delivering proteins with fluorophores attached to a specific site into live cells, there have been studies that have successfully delivered modified proteins into live cells while retaining their full function[22,25]. To illustrate the significance, we applied our setup to determine the orientation of helix six in membrane embedded Bax and address a discrepancy in the determination of this pore-forming helix. This discrepancy can be attributed to a changing membrane environment. We demonstrated that the added versatility in our method allowed probing of structural conformation at precise locations on a time scale conductive to studying dynamic membrane environments. Our approach can be utilized to investigate a variety of other systems that encounter changing membrane morphology.

Supplementary Material

Refer to Web version on PubMed Central for supplementary material.

ACKNOWLEDGMENT

We thank Dr. Yu Wang for providing the tBid and Dr. Greg Piszczek of the Biophysics Core Facility, Biochemistry and Biophysics Center, NHLBI, for helpful discussions. The Intramural Research Program of the National Heart Lung and Blood Institute (NHLBI) of the National Institutes of Health (NIH) supported this work.

REFERENCES

1. Jennings ML. Topography of Membrane Proteins. Annu. Rev. Biochem. 1989; 58:999–1027. [PubMed: 2673027]
2. van Geest M, Lolkema JS. Membrane Topology and Insertion of Membrane Proteins: Search for Topogenic Signals. Microbiol. Mol. Biol. Rev. 2000; 64:13–33. [PubMed: 10704472]
3. Wimley WC, White SH. Determining the Membrane Topology of Peptides by Fluorescence Quenching. Biochemistry. 2000; 39:161–170. [PubMed: 10625491]
4. Ladokhin AS, Isas JM, Haigler HT, White SH. Determining the Membrane Topology of Proteins: Insertion Pathway of a Transmembrane Helix of Annexin 12. Biochemistry. 2002; 41:13617–13626. [PubMed: 12427023]
5. Zhu Q, Casey JR. Topology of Transmembrane Proteins by Scanning Cysteine Accessibility Mutagenesis Methodology. Methods. 2007; 41:439–450. [PubMed: 17367716]
6. González JE, TSIEN RY. Voltage Sensing by Fluorescence Resonance Energy Transfer in Single Cells. Biophysical Journal. 1995; 69:1272–1280. [PubMed: 8534797]
7. González JE, TSIEN RY. Improved Indicators of Cell Membrane Potential That Use Fluorescence Resonance Energy Transfer. Chem. Biol. 1997; 4:269–277. [PubMed: 9195864]
8. Chanda B, Blunck R, Faria LC, Schweizer FE, Mody I, Bezanilla F. A Hybrid Approach to Measuring Electrical Activity in Genetically Specified Neurons. Nat. Neurosci. 2005; 8:1619–1626. [PubMed: 16205716]
9. Chanda B, Kwame Asamoah O, Blunck R, Roux B, Bezanilla F. Gating Charge Displacement in Voltage-Gated Ion Channels Involves Limited Transmembrane Movement. Nature. 2005; 436:852–856. [PubMed: 16094369]
10. Groulx N, Juteau M, Blunck R. Rapid Topology Probing Using Fluorescence Spectroscopy in Planar Lipid Bilayer: the Pore-Forming Mechanism of the Toxin Cry1Aa of Bacillus Thuringiensis. The Journal of General Physiology. 2010; 136:497–513. [PubMed: 20974771]
11. Frolov VA, Shnyrova AV, Zimmerberg J. Lipid Polymorphisms and Membrane Shape. Cold Spring Harbor Perspectives in Biology. 2011; 3:a004747. [PubMed: 21646378]
12. Czabotar PE, Lessene G, Strasser A, Adams JM. Control of Apoptosis by the BCL-2 Protein Family: Implications for Physiology and Therapy. Nat Rev Mol Cell Biol. 2013; 15:49–63. [PubMed: 24355989]
13. Westphal D, Dewson G, Menard M, Frederick P, Iyer S, Bartolo R, Gibson L, Czabotar PE, Smith BJ, Adams JM, et al. Apoptotic Pore Formation Is Associated with in-Plane Insertion of Bak or Bax Central Helices Into the Mitochondrial Outer Membrane. Proc. Natl. Acad. Sci. U.S.A. 2014; 111:E4076–E4085. [PubMed: 25228770]
14. Gahl RF, He Y, Yu S, Tjandra N. Conformational Rearrangements in the Pro-Apoptotic Protein, Bax, as It Inserts Into Mitochondria: a CELLULAR DEATH SWITCH. Journal of Biological Chemistry. 2014; 289:32871–32882. [PubMed: 25315775]
15. Bleicken S, Jeschke G, Stegmueller C, Salvador-Gallego R, García-Sáez AJ, Bordignon E. Structural Model of Active Bax at the Membrane. Molecular Cell. 2014; 56:496–505. [PubMed: 25458844]
16. DiFranco M, Capote J, Vergara JL. Optical Imaging and Functional Characterization of the Transverse Tubular System of Mammalian Muscle Fibers Using the Potentiometric Indicator Di-8-ANEPPS. J. Membr. Biol. 2005; 208:141–153. [PubMed: 16645743]

17. Turnbull RJ. Letter: an Alternate Explanation for the Permeability Changes Induced by Electrical Impulses in Vesicular Membranes. J. Membr. Biol. 1973; 14:193–196. [PubMed: 4774546]

18. Lojewska Z, Farkas DL, Ehrenberg B, Loew LM. Analysis of the Effect of Medium and Membrane Conductance on the Amplitude and Kinetics of Membrane Potentials Induced by Externally Applied Electric Fields. Biophysical Journal. 1989; 56:121–128. [PubMed: 2752081]

19. Kotnik T, Miklavcic D. Analytical Description of Transmembrane Voltage Induced by Electric Fields on Spheroidal Cells. Biophysical Journal. 2000; 79:670–679. [PubMed: 10920001]

20. Schote U, Seelig J. Interaction of the Neuronal Marker Dye FM1-43 with Lipid Membranes. Thermodynamics and Lipid Ordering. Biochim. Biophys. Acta. 1998; 1415:135–146.

21. Henkel AW, Lübke J, Betz WJ. FM1-43 Dye Ultrastructural Localization in and Release From Frog Motor Nerve Terminals. Proc. Natl. Acad. Sci. U.S.A. 1996; 93:1918–1923. [PubMed: 8700859]

22. Gahl RF, Tekle E, Tjandra N. Single Color FRET Based Measurements of Conformational Changes of Proteins Resulting From Translocation Inside Cells. Methods. 2014; 66:180–187. [PubMed: 23872323]

23. Lovell JF, Billen LP, Bindner S, Shamas-Din A, Fradin C, Leber B, Andrews DW. Membrane Binding by tBid Initiates an Ordered Series of Events Culminating in Membrane Permeabilization by Bax. Cell. 2008; 135:1074–1084. [PubMed: 19062087]

24. Annis MG, Dlugosz PJ, Cruz-Aguado JA, Penn LZ, Leber B, Andrews DW. Bax Forms Multispanning Monomers That Oligomerize to Permeabilize Membranes During Apoptosis. EMBO J. 2005; 24:2096–2103. [PubMed: 15920484]

25. Sakon JJ, Weninger KR. Detecting the Conformation of Individual Proteins in Live Cells. Nat Meth. 2010; 7:203–205.

HIGHLIGHTS

- Determining the orientation of macromolecules in a membrane is very difficult.
- Integrating a confocal microscope with a pulsed electric field is a powerful solution.
- This setup can determine the orientation of molecules rapidly with spatial specificity.
- The orientation of a transmembrane helix in a pore forming protein was determined.
- This approach can be applied to a variety of systems including live cells.

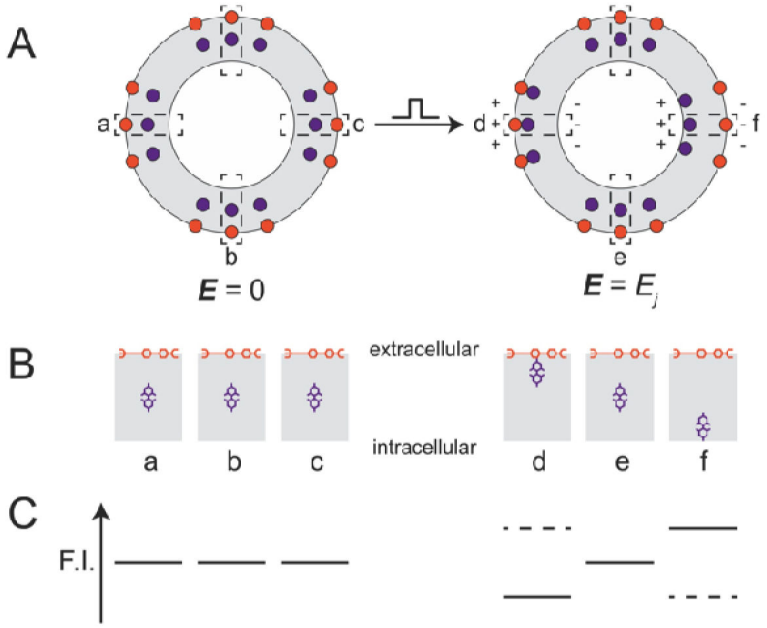

Figure 1.

(A, *left)* Equilibrium distribution of a donor fluorophore (red dot) on the outer membrane leaflet and dipicrylamine (DPA –purple dot) in the absence of an external field, E=0. (*right*) After the application of a pulsed electric field, $E=E_j$, DPA preferentially migrates to a leaflet. (B) Change in the distance between the fluorophone (red objects) and DPA (blue objects) in various locations as indicated in panel A before (a-c) and after (d-f) the application of the pulsed electric field. (C) The fluorescence intensity (F.I.) of the fluorophore will be affected by changes in the DPA location due to FRET. When its distance to the DPA is closer (as in d), the intensity goes down. An increase in its intensity, however can be observed, as DPA moves further (as in f) from its equilibrium position. Dotted lines show changes in intensity if the fluorophore was on the opposite leaflet.

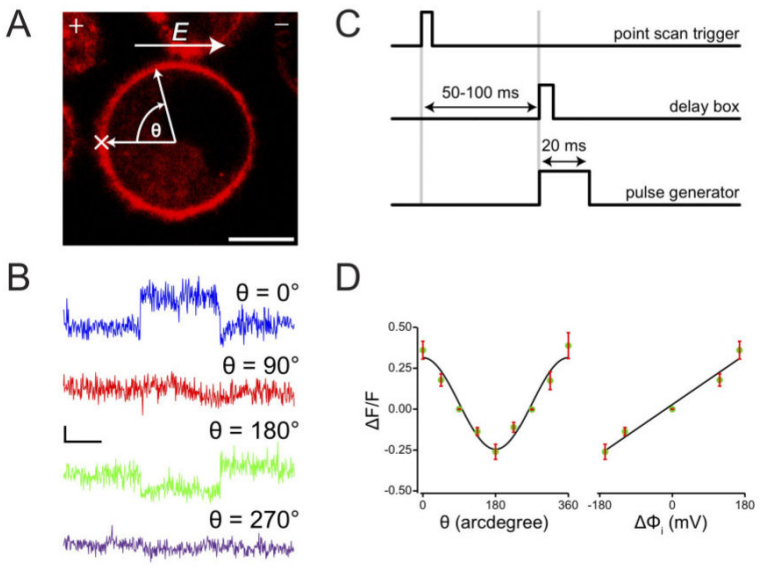

Figure 2.

(A) Fluorescence image of a PC12 cell stained with Di-8-ANEPPS. The polarity of the electric field *E*, is indicated by "+" and "−" signs. Fluorescent signals were collected at certain points around the membrane of the cell at an angle, θ, relative to a reference point, "×". Scale bar = 10 μm (B) Single trace optical signals at select positions on the membrane. Horizontal scale bar = 10 ms, and vertical scale bar = 20% in Δ*F*/*F*. (C) Timing diagram for signal acquisition and pulse application. (D) Δ*F*/*F* along the cell membrane for an applied field of constant amplitude at different orientations relative to the electric field. An angular dependence of Δ*F*/*F* was observed (*left*) as well as a 16.9% change in signal response per 100 mV of induced transmembrane potential, $\Delta\Phi_i$ (*right*). Error bars represent standard errors, n=3.

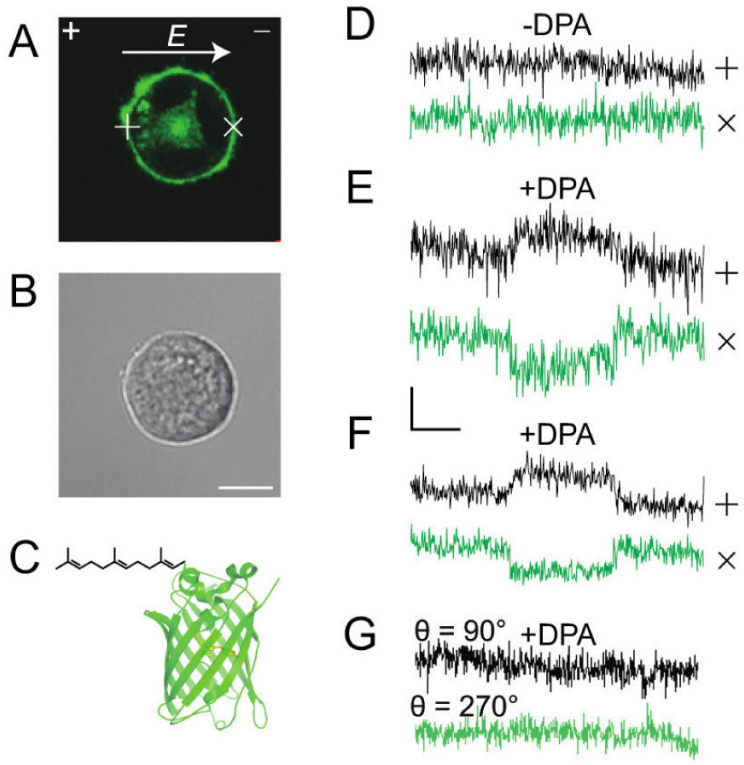

Figure 3.

(A) Fluorescence image of a PC12 cell transfected with a plasmid encoding for farnesylated monomeric enhanced green fluorescent protein, mEGFP-F, where the farnesyl moiety targets GFP to the inner leaflet of the cell membrane. The direction and polarity of the electric field, *E*, is indicated by the arrow and the "+" and "−" sign, respectively. (B) Bright field image of A. Scale bar = 10 μm. (C) Structure of mEGFP-F. (D-G) Data collected at positions marked (+), (anodic-facing) and (x), (cathodic-facing) hemispheres of the cell membrane. No effect on the fluorescence is observed if DPA is not added to the membrane (D), but opposite changes in the signal is observed when DPA is incorporated into the membrane as expected (E). An average of three independent traces of fluorescence intensity (F) shows consistent FRET effect confirming the location of the mEGFP-F on the inner membrane leaflet and consequently an electric field oriented orthogonal to the movement between leaflets shows no change in signal even if DPA is present (G).

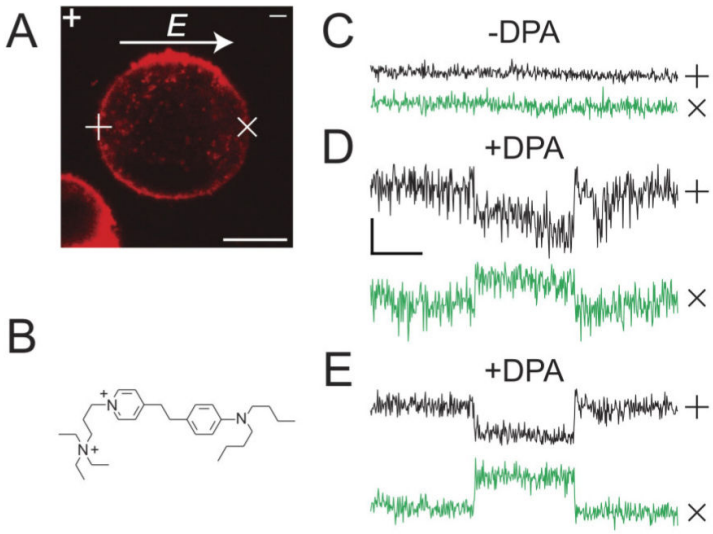

Figure 4.

(A) Fluorescence image of PC12 cell labeled with 1 μM of FM1-43. Data are collected at positions marked (+) and (×) on the cell membrane. Scale bar = 10 μm. The polarity of the electric field, *E*, is indicated by the "+" and "−" signs. (B) Structure of FM1-43. (C) Optical response in the absence of DPA. (D) Optical response in the presence of 10 μM DPA. (E) Averaged signal for experimental conditions as in [D], n=3. ***E***=166 V/cm, pulse width = 20 ms in traces [C]-[E].

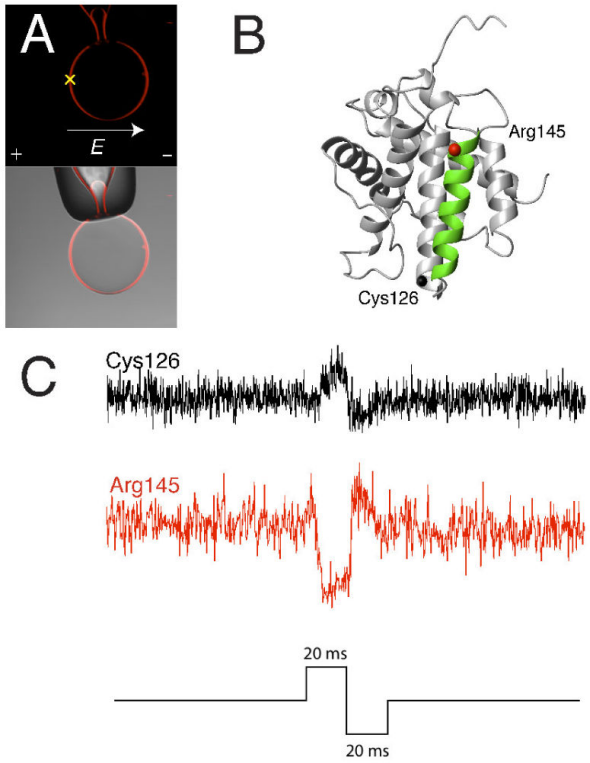

Figure 5.

(A) Wide-field image of a GUV that contains tBid, DPA, and fluorescence labeled Bax held in place by a Cell Holder Unit. The "×" indicates the approximate region where the fluorescent signal on the membrane was acquired. (B) Structure of Bax (PDBID: 1F16) where the Cα atoms of Cys126 (black) and Arg145 (red) are shown on helix six (green). (C) Signals from a point scan in A for Cys126 (Black) and Arg145Cys (Red). The two electric pulses that give rise to these signals is drawn below.